Article No. jmbi.1999.2589 available online at http://www.idealibrary.com on IDEAL J. Mol. Biol. (1999) 287, 145–161

JMB

Protein Conformational Changes in the Bacteriorhodopsin Photocycle

Sriram Subramaniam[1]*, Martin Lindahl[1], Per Bullough[1], A. R. Faruqi[1] Jörg Tittor[2], Dieter Oesterhelt[2], Leonid Brown[3], Janos Lanyi[3] and Richard Henderson[1]*

[1]*MRC Laboratory for Molecular Biology, Cambridge England*

[2]*Max-Planck Institute for Biochemistry, Martinsried Germany*

[3]*University of California Irvine, CA, USA*

**Corresponding authors*

We report a comprehensive electron crystallographic analysis of conformational changes in the photocycle of wild-type bacteriorhodopsin and in a variety of mutant proteins with kinetic defects in the photocycle. Specific intermediates that accumulate in the late stages of the photocycle of wild-type bacteriorhodopsin, the single mutants D38R, D96N, D96G, T46V, L93A and F219L, and the triple mutant D96G/F171C/F219L were trapped by freezing two-dimensional crystals in liquid ethane at varying times after illumination with a light flash. Electron diffraction patterns recorded from these crystals were used to construct projection difference Fourier maps at 3.5 Å resolution to define light-driven changes in protein conformation.

Our experiments demonstrate that in wild-type bacteriorhodopsin, a large protein conformational change occurs within ~1 ms after illumination. Analysis of structural changes in wild-type and mutant bacteriorhodopsins under conditions when either the M or the N intermediate is preferentially accumulated reveals that there are only small differences in structure between M and N intermediates trapped in the same protein. However, a considerably larger variation is observed when the same optical intermediate is trapped in different mutants. In some of the mutants, a partial conformational change is present even prior to illumination, with additional changes occurring upon illumination. Selected mutations, such as those in the D96G/F171C/F219L triple mutant, can sufficiently destabilize the wild-type structure to generate almost the full extent of the conformational change in the dark, with minimal additional light-induced changes. We conclude that the differences in structural changes observed in mutants that display long-lived M, N or O intermediates are best described as variations of one fundamental type of conformational change, rather than representing structural changes that are unique to the optical intermediate that is accumulated. Our observations thus support a simplified view of the photocycle of wild-type bacteriorhodopsin in which the structures of the initial state and the early intermediates (K, L and M_1) are well approximated by one protein conformation, while the structures of the later intermediates (M_2, N and O) are well approximated by the other protein conformation. We propose that in wild-type bacteriorhodopsin and in most mutants, this conformational change between the M_1 and M_2 states is likely to make an important contribution towards efficiently switching proton accessibility of the Schiff base from the extracellular side to the cytoplasmic side of the membrane.

Keywords: electron crystallography; seven-helix membrane protein; proton pump; conformational change; trapped intermediates

Present addresses: S. Subramaniam, Laboratory of Biochemistry, National Cancer Institute, Bethesda, MD, USA; M. Lindahl, Max Planck Institute for Biophysics, Frankfurt, Germany; P. Bullough, Krebs Institute for Biomolecular Research, University of Sheffield, Sheffield, England.

E-mail address of the corresponding author: sriram@mrc-lmb.cam.ac.uk or rh15@mrc-lmb.cam.ac.uk

0022-2836/99/110145–17 $30.00/0

Introduction

Isomerization of retinal by light is the first step in the transduction of light energy by proteins in the rhodopsin family. In bacteriorhodopsin, light-induced retinal isomerization from the all-*trans* to the 13-*cis* configuration (Tsuda *et al*., 1980; Stoeckenius *et al*., 1979) triggers changes in protein conformation which result in three important stages in the photocycle: (i) the release of a proton into the extracellular medium; (ii) the uptake of a proton from the cytoplasmic medium; and (iii) the thermal re-isomerization of retinal to the starting all-*trans* configuration. These conformational changes are reflected as changes in the visible region of the absorption spectrum, as evidenced by the sequential formation and decay of the optical intermediates J, K, L, M, N, and O (Lozier *et al*., 1975; Ebrey, 1993). Spectroscopic studies of wild-type bacteriorhodopsin have shown that the release of a proton ($\tau \sim 50$ μs) into the extracellular medium coincides with the formation of the M intermediate (Grzesiek & Dencher, 1986). Detailed spectroscopic and biochemical analyses of many site-specific mutants (Butt *et al*., 1989; Otto *et al*., 1990; Subramaniam *et al*., 1990) have established that the presence of a deprotonated carboxylate group at residue 85 is essential for effective proton release. The path of the proton from the Schiff base to the external medium is lined by residues Asp85, Arg82, Asp212, Glu204 and Glu194. Replacements of each one has measurable effects on the kinetics and/or efficiency of proton release. However, none of these residues are completely indispensable for the functioning of the proton pump, and indeed it has been proposed that a complex H-bonded network involving these residues and bound water molecules is responsible for proton conduction (Rammelsberg *et al*., 1998). Together, these findings suggest that the proton released from the Schiff base can reach the extracellular medium at varying speeds and through multiple routes, and that the most likely route need not be the same in different mutants. Similar mutagenesis studies have established that the presence of a carboxylate group at residue 96 is important for rapid reprotonation of the Schiff base (Gerwert *et al*., 1989; Marinetti *et al*., 1989; Tittor *et al*., 1989; Otto *et al*., 1989; Miller & Oesterhelt 1990). Reprotonation of the Schiff base by Asp96 is reflected by the spectroscopically detectable conversion of the M intermediate to the N intermediate. Asp96 is reprotonated from the cytoplasmic medium, initiating formation of the O intermediate. Amino acid replacements of residues that are in the vicinity of the reprotonation pathway such as Thr46, Phe171 and Phe219 result in accumulation of the N intermediate (Brown *et al*., 1994a; Kamikubo *et al*., 1996), while replacement of Leu93 or Val49 result in an accumulation of the O intermediate (Delaney *et al*., 1995). In the final phase of the photocycle, retinal is thermally re-isomerized from the 13-*cis* to the all-*trans* configuration (Smith *et al*., 1983; Delaney *et al*., 1995; Kandori *et al*., 1997). At 25 °C, the photocycle is complete in about 10 ms.

A combination of previous neutron (Dencher *et al*., 1989), X-ray (Koch *et al*., 1991; Kamikubo *et al*., 1997) and electron diffraction studies (Subramaniam *et al*., 1993, 1997; Vonck, 1996), have provided strong evidence that the transmembrane regions of bacteriorhodopsin undergo significant light-induced changes in conformation during the course of the photocycle. In our earlier work, we reported projection structural changes in wild-type bacteriorhodopsin and the D96G mutant trapped 10 or 20 ms after illumination at 5 °C, and in the L93A mutant trapped five seconds after illumination at 5 °C. Based on these projection maps we concluded that the main structural change in the photocycles of both proteins was largely localized to the central four helices lining the proton channel (F, G, B and C; see Figure 1(c)). Based on the relative disposition of the positive and negative peaks in the projection difference maps, and from a low-resolution three-dimensional difference map, we proposed that the main features of the structural change were likely to be an ordering of helix G at the cytoplasmic end and an outward tilt of helix F, with Pro186 likely to serve as a ''hinge'' residue. An unresolved aspect of these difference maps was that while the difference Fourier maps for wild-type bacteriorhodopsin, the D96G mutant and the L93A mutant were qualitatively similar, there were nevertheless noticeable differences in the relative magnitudes of the peaks observed in different regions of the protein. Thus, in wild-type bacteriorhodopsin, the strongest peak was near helix G, with progressively weaker peaks near helices B, F and C, respectively. In the D96G mutant, the peaks near helices F and G were of a similar magnitude, and weaker peaks were observed near helices B and C, while in the L93A mutant the peaks near helices G and C were of a similar magnitude, with weaker peaks near helix F and B.

The differences observed between wild-type bacteriorhodopsin and the mutants could have two origins. One potential source is the difference in composition of intermediates trapped in wild-type and the mutant. Under the conditions of our experiment, a mixture of M and N intermediates is expected to be trapped in wild-type bacteriorhodopsin (Varo & Lanyi, 1991b). In the D96G mutant, the only optically distinguishable intermediate present is the M intermediate. Based on FTIR studies with the D96N mutant, Sasaki *et al*. (1992) proposed that the M intermediate in the photocycle of this mutant (which they named the M_N intermediate) has protein structural features more closely resembling the N intermediate of the photocycle of wild-type bacteriorhodopsin. If this interpretation also holds true for the D96G mutant, it is possible that the structural features observed in the D96G mutant are more representative of the N intermediate. Similarly, detailed optical spectroscopic studies

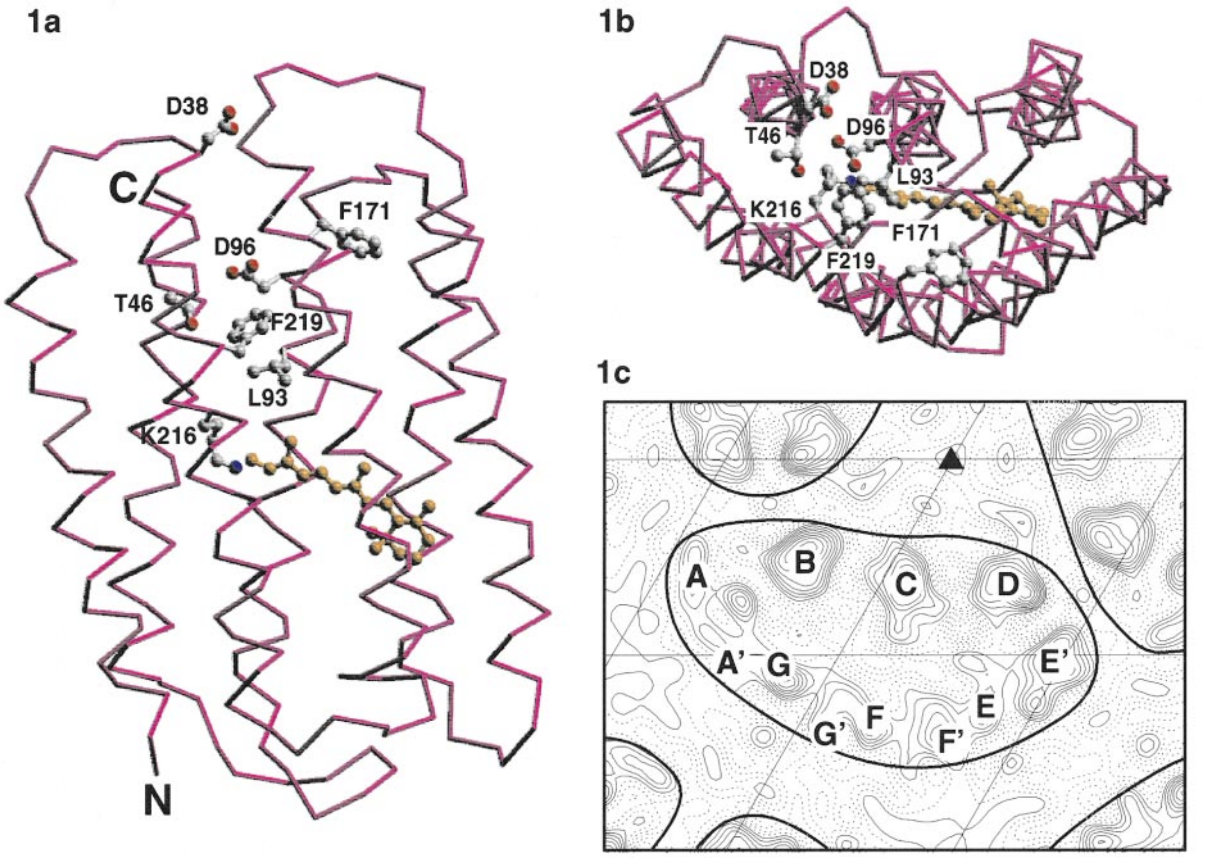

Figure 1. (a) Ribbon representation and (b) projection view from the cytoplasmic side of the three-dimensional structure of bacteriorhodopsin as reported by Grigorieff *et al.* (1996). (c) Two-dimensional projection Fourier map of wild-type bacteriorhodopsin at 3.5 Å resolution, identifying locations of the seven transmembrane helices. The filled triangle indicates the location of the 3-fold axis. The grid bars are spaced at 20.81 Å, which is one-third the length of the unit cell. The continuous lines around the densities show the approximate boundaries of individual molecules in the lattice.

with the L93A mutant have shown that only the O intermediate is expected to be trapped under the conditions of our experiment (Delaney *et al.*, 1995). Therefore, one possible explanation for the variations in the projection maps is that the structural features observed for wild-type bacteriorhodopsin are more representative of the M intermediate, while those observed in the D96G and L93A mutants are representative of the N and O intermediates, respectively. An alternative possibility is that variations in the difference maps are primarily due to the energetic consequences of replacing Asp96 by Gly, or Leu93 by Ala. The presence of these mutations could cause a difference in conformational flexibility and in helix-helix interactions, especially in the cytoplasmic half of the membrane-embedded portion of the protein, thereby causing variations in the extent of the conformational change in different regions of the protein. In this scenario, the structural changes observed in wild-type bacteriorhodopsin, D96G and L93A mutants would be best described as variations of one basic type of conformational change, rather than representing structural changes that are unique to the M, N or O intermediates.

To assess whether one or both of the above mechanisms are responsible for the differences observed between wild-type bacteriorhodopsin and the D96G mutant, we have calculated difference Fourier maps using diffraction patterns recorded from crystals of wild-type bacteriorhodopsin under conditions where either the M or the N intermediate is the predominant intermediate present. To investigate whether structural changes in the D96G mutant are significantly influenced by energetic consequences of the Asp96 $\rightarrow$ Gly mutation, we have compared structural changes in the D96G mutant with those in the D96N mutant. We have also calculated difference Fourier maps using diffraction patterns recorded from illuminated crystals of the F219L mutant in which there is a clear kinetic separation between the M and the N intermediates. Finally, we have also studied three other mutants (D38R, T46V and the D96G/F171C/F219L triple mutant) in which the photocycle is significantly slowed down, resulting in the accumulation of either M-like or N-like intermedi-

ates. Figure 1(a) and 1(b) show the locations of the residues replaced in the various mutants described above, while Figure 1(c) shows a projection map of wild-type bacteriorhodopsin to serve as a guide in interpreting the locations of peaks in the difference Fourier maps shown in subsequent Figures.

Results

Structural changes in wild-type bacteriorhodopsin

Figure 2(a) shows a difference Fourier map illustrating structural changes in wild-type bacteriorhodopsin (pH 6, 5 °C) ~ 1 ms into the photocycle, which represents the earliest time that we were able to trap the crystals after illumination (see Methods section for experimental details on trapping intermediates at this early time). Comparison of this difference map with those obtained at later times in the photocycle (Figure 2(b)-(e)) shows that all of the main features in the difference maps seen at times as late as 35 ms are also present at 1 ms. As previously reported for intermediates trapped at 10 and 20 ms after illumination (Subramaniam *et al*., 1993), the strongest peak in all of the maps is near helix G, with progressively weaker features near helices B and F, and C. We therefore conclude that the main conformational change in the photocycle has already occurred within 1 ms after illumination.

Spectroscopic studies (Varo & Lanyi, 1991b) have shown that at 5 °C, and at times between 1 ms and 35 ms, an equilibrium mixture of M and N intermediates is accumulated. At 1 ms, mostly the M intermediate is present (> ~ 90 %), while at 35 ms the intermediate composition is only ~2:1 ratio in favor of the M intermediate. A double difference map between the maps obtained at early and late times may therefore contain any additional features that are unique to the N intermediate. Such a double difference map comparing changes at 35 ms *versus* changes at 1 ms is shown in Figure 2(f). The positive and negative peaks in this map are ~twofold above the noise level, with features detectable in the vicinity of helices F and G. It is important to note that a quantitative comparison of the difference maps at early and late times is somewhat difficult because of possible variations in illumination conditions depending on the speed of the plunger (see Methods). With this caveat in mind, we conclude that in addition to the main structural change that occurs early in the photocycle, a further smaller additional change may occur on a time-scale corresponding to the conversion of the M to the N intermediate. From an extrapolation of our earlier work, it seems likely that these additional changes would also be localized to the cytoplasmic domain and could represent a further ''widening'' of the proton channel by the movement of helix F.

Analysis of structural changes at pH 9.5 provides a further insight into this problem. Figure 3(a) shows a difference Fourier map illustrating structural changes in wild-type bacteriorhodopsin 35 ms after illumination at 5 °C at pH 9.5. Spectroscopic studies (Ames & Mathies, 1990; Pfefferle *et al*., 1991) have suggested that under these conditions, an equilibrium mixture of M and N intermediates is accumulated; however, in contrast to the situation at pH 6, the equilibrium favors population of the N intermediate by a ratio of ~2:1. Differences between the maps in Figure 2(e) (pH 6, 35 ms) and Figure 3(a) (pH 9.5, 35 ms) could therefore reflect structural differences between the M and N intermediates. Comparison of the difference maps at pH 6 and 9.5 reveals that they are fundamentally similar with respect to the location of the various positive and negative peaks, but that almost all of the peaks are stronger in the map at pH 9.5. Because of the slower decay of the M and N intermediates at pH 9.5 as compared to pH 6, a higher ''occupancy'' of the intermediates states (by a factor of about 1.2) is expected at pH 9.5. The stronger peaks seen at pH 9.5 are therefore completely consistent with this prediction.

To estimate any differences in detail between the maps obtained at the two pH values, a double difference map was calculated (Figure 3(b)). Inspection of the double difference map reveals that although small, there are detectable peaks in the map near helices G, F and B. We conclude that at pH 9.5, the amplitude of the structural change is larger than that which would be expected solely on the basis of the slower photocycling time. This increase could be interpreted as an intrinsic difference between the M intermediate (in which the Schiff base is deprotonated, and proton donor Asp96 is protonated) and the N intermediate (in which the Schiff base is protonated and Asp96 is deprotonated). As with the conclusion above regarding additional changes at later *versus* early times (Figure 2(f)), it seems likely that the additional changes seen at higher pH could also represent a further ''widening'' of the cytoplasmic proton channel.

Comparison of structural changes in the D96G and D96N mutants

The small differences observed between structural changes at pH 6 and pH 9.5 appear to be insufficient to account for the differences previously observed (Subramaniam *et al*., 1993) between structural changes in wild-type bacteriorhodopsin and the D96G mutant. To establish whether the energetic consequences of the Asp96 → Gly mutation influence the nature of the light-driven conformational change, we have compared conformational changes in the D96G mutant with a mutant (D96N) in which Asp96 is replaced by the isosteric residue, asparagine. Figure 4(a) and (b) show projection Fourier maps obtained for the D96G mutant (pH 6) at 1 ms and 20 ms after illumination at 5 °C. The two maps are very similar to each other and, in turn, are similar to the previously reported map

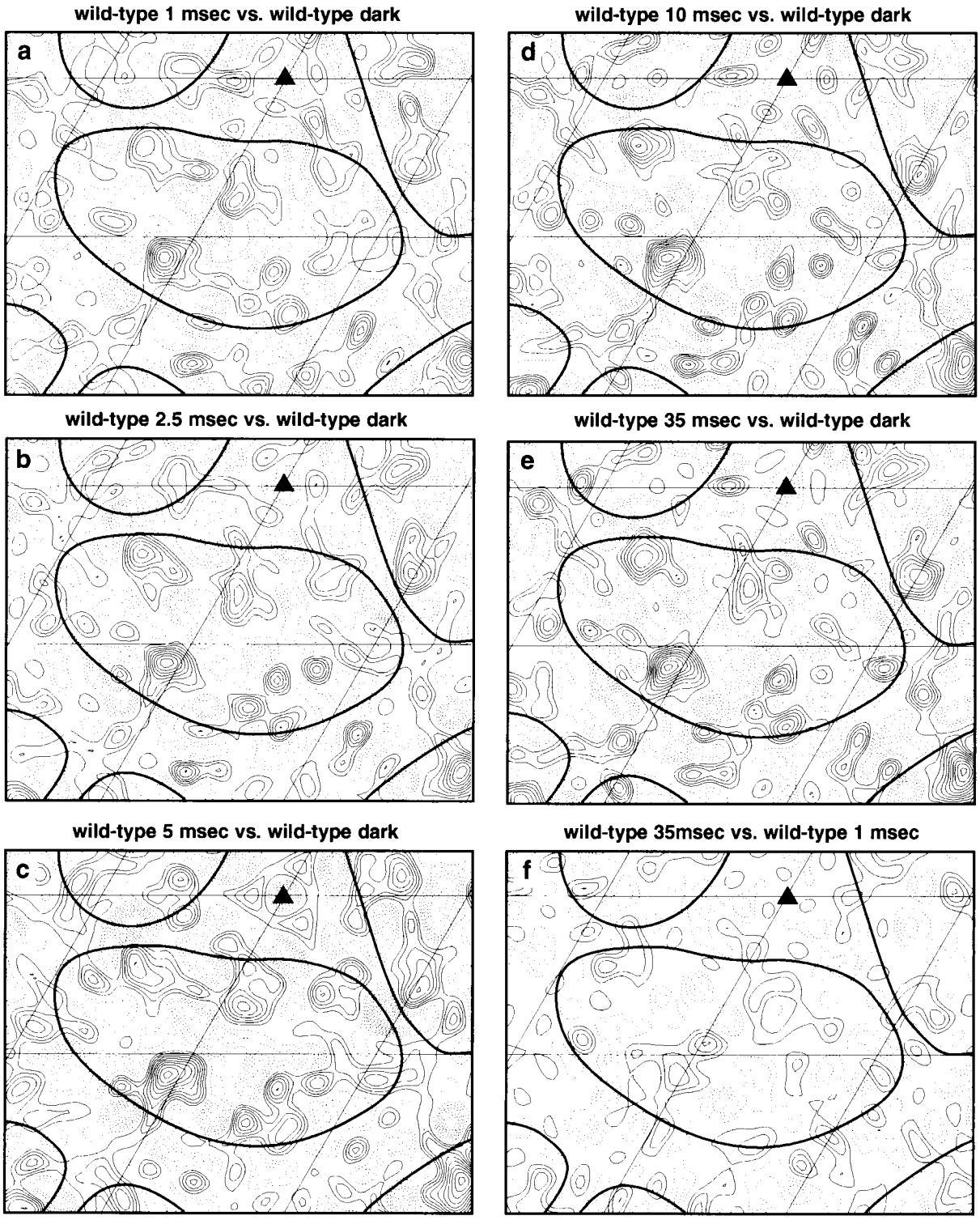

Figure 2. Difference maps showing structural changes in crystals of wild-type bacteriorhodopsin at different times after illumination at pH 6 and at 5 °C using unilluminated crystals of wild-type bacteriorhodopsin under the same conditions as a reference. The times between illumination and freezing are (a) 1 ms, (b) 2.5 ms, (c) 5 ms, (d), 10 ms and (e) 35 ms. The maps show that similar features are observed at early and late times in the photocycle. The slightly lower peak height observed in the 1 ms map is due, at least in part, to a lower occupancy of the intermediate since the transit time of the grid across the beam (~0.3 ms) is significantly shorter than the width of the flash (~1 ms). (f) Double difference map comparing changes at 35 ms to those at 1 msec shows peaks in the vicinity of helices F, G and B. The continuous line in each difference map has been drawn to show the approximate boundary of an individual molecule in the lattice. Difference maps in this Figure and in all subsequent Figures have been contoured at the same interval, which, in turn, is one-tenth of the contour interval used for the native projection map in Figure 1(c). Difference maps in (b), (d) and (e) are at 3.5 Å resolution, and the ones in (a), (c) and (f) are at 4.0 Å resolution.

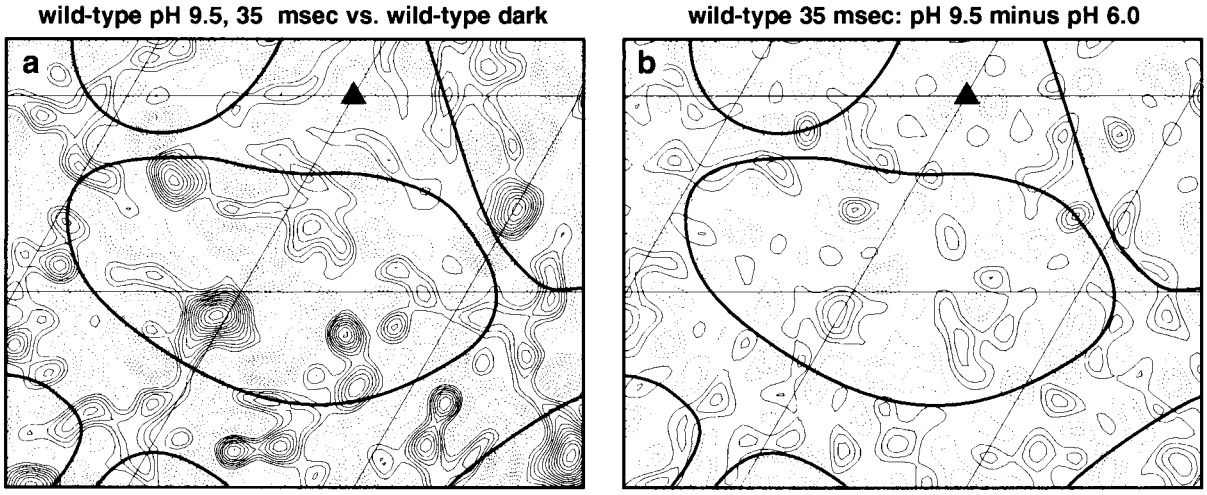

Figure 3. (a) Difference map showing structural changes in crystals of wild-type bacteriorhodopsin 35 ms after illumination at pH 9.5 and at 5 °C using unilluminated crystals of wild-type bacteriorhodopsin at pH 6 as a reference. (b) Double difference map comparing structural changes at pH 9.5 to those at pH 6 (both measured at 35 ms after illumination) shows features in the vicinity of helices F, G and B, similar to those in the double difference map observed in Figure 2(f).

(Figure 4(c)) using crystals trapped 20 ms after illumination at room temperature (Subramaniam *et al*., 1993). Spectroscopic studies have shown that only the M optical intermediate is accumulated in the D96G mutant over this time and temperature range.

Figure 4(d) and (e) show projection difference maps for the D96N mutant 10 ms after illumination (at 5 °C) at pH 6 and pH 9.5, respectively. The photocycle of the D96N mutant is very similar to that of the D96G mutant (Tittor *et al*., 1989) and spectroscopic studies have shown that only the M intermediate is accumulated at times greater than about 1 ms (Miller & Oesterhelt, 1990). As noted earlier, Sasaki *et al*. (1992) have argued previously that the amide I region of the FTIR spectrum of this M-like state is more analogous to the N rather than the M intermediate of the wild-type photocycle. Our experiments show that the difference maps obtained at both pH values (Figure. 4(d) and (e)) are remarkably similar to the difference map obtained for wild-type bacteriorhodopsin at pH 9.5 (Figure 3(a)), and noticeably different from the difference maps obtained for the D96G mutant (Figure 4(a)-(c)). In particular, although in both D96N and D96G mutants there are peaks near helices G, F and B, the relative amplitudes and shapes of each of these features are clearly different. The similarity of the wild-type and D96N difference maps is clearly established by the double difference map calculated in Figure 4(f), which has no significant features above the noise level.

Structural changes at early and late times in the F219L mutant

The experiments presented so far demonstrate that there are only small differences in structure between M and N intermediates in the photocycle of wild-type bacteriorhodopsin, and that the structural changes previously observed between wild-type bacteriorhodopsin and the D96G mutant can be explained in large part by the energetic consequences of the Asp96 → Gly mutant. A more stringent estimate of the structural change between the M and N intermediates would be possible if conditions were identified in which there is a clear kinetic separation of the M and N intermediates upon illumination at the same temperature and pH conditions. The F219L mutant is useful in this regard, since in the photocycle of this mutant the decay of the M intermediate is about 100-fold faster than the decay of the N intermediate (Figure 5). We have therefore calculated difference Fourier maps to analyze structural changes in this mutant at early times (6 ms) close to the peak concentration of M, and at later times (35 ms) when most of the M intermediate has decayed to generate the N intermediate.

Figure 6(a) shows a control difference map comparing the structure of the unilluminated F219L mutant to that of unilluminated wild-type bacteriorhodopsin. Noticeable structural changes in the vicinity of helices B, C and G are observed, indicating mutation-induced perturbations of the structure even in the absence of illumination. A similar observation was reported for the L93A mutant (Subramaniam *et al*., 1997), in which a long-lived O intermediate is accumulated during the photocycle. Figure 6(b) and (c) show difference Fourier maps illustrating light-induced changes in the F219L mutant when trapped at 6 ms (Figure 6(b)) or at 35 ms (Figure 6(c)) using the unilluminated mutant as a reference. It is clear that the structural changes at both times are very similar, with a marginally larger extent of the structural change at the later time. The experiments with the F219L mutant therefore provide independent confirmation for the

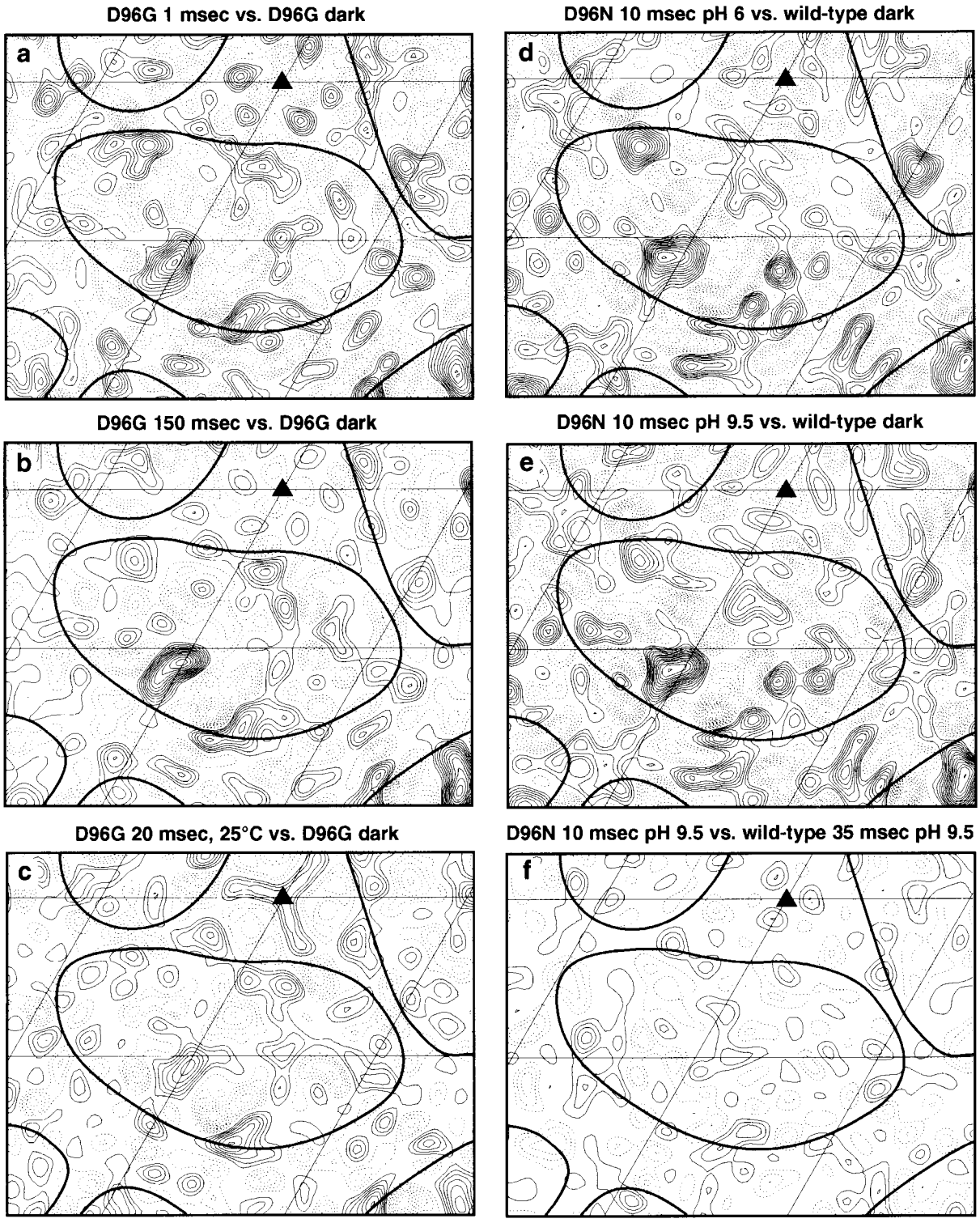

Figure 4. Difference maps showing structural changes in crystals of the D96G mutant (a) 1 ms and (b) 20 ms after illumination at pH 6 and at 5 °C, using unilluminated crystals of the D96G mutant as a reference. The maps are not different when wild-type bacteriorhodopsin is used as a reference (data not shown), as expected based on our previous finding (Subramaniam *et al*., 1993) that the structure of the D96G mutant in the unilluminated state is similar to that of unilluminated wild-type bacteriorhodopsin. (c) Difference map showing structural changes in crystals of the D96G mutant 20 ms after illumination at pH 8.5 and at 25 °C, using unilluminated crystals of the D96G mutant as a reference (data taken from Subramaniam *et al*., 1993). The more pronounced features in the 5 °C maps are due mainly to the higher occupancy of the intermediate state. In the new experiments ((a) and (b)), higher light intensities were incident on the grid since a 570 nm cutoff filter was used, as compared to the previous experiments, in which a 550 (±20) nm interference filter was used. Difference maps showing structural changes in crystals of the D96N mutant 10 ms after illumination at (d) pH 6 and (e) pH 9.5 at 5 °C, using unilluminated crystals of wild-type bacteriorhodopsin at pH 6 as a reference. (f) Double difference map comparing structural changes in the D96N mutant 10 ms after illumination, and at pH 9.5 to those in wild-type bacteriorhodopsin 35 msec after illumination, also at pH 9.5. The features in this double difference map are near the noise level, implying that structural changes in the D96N mutant are closely comparable to those in wild-type bacteriorhodopsin.

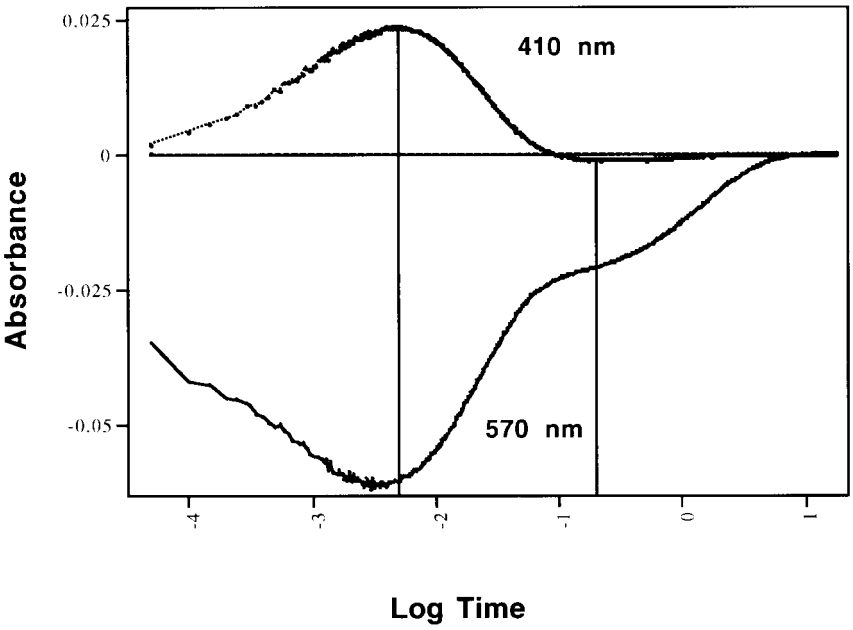

Figure 5. Transient absorption changes after flash excitation of membrane fragments of the F219L mutant at 5 °C in 200 mM sodium chloride and 10 mM phosphate buffer at pH 7. Absorbance changes at 410 nm provide a marker for the time-dependent changes in the concentration of the M intermediate, which peaks at ~6 ms. Absorbance changes at 570 nm provide a marker for time-dependent changes in the concentration of the N intermediate, which peaks at ~200 ms. The absorbance at 570 nm contains contributions from both the initial bacteriorhodopsin state ($\lambda_{max} \sim$ 570 nm) and the N intermediate ($\lambda_{max} \sim 560$ nm). Since the extinction coefficient of the N intermediate is less than that of bacteriorhodopsin, the decay of the N intermediate is seen as a transient with net negative absorbance values.

principal conclusions drawn from analysis of structural changes at the M and N stages of the photocycle of wild-type bacteriorhodopsin. Figure 6(d) shows a difference map illustrating structural changes in the F219L mutant using unilluminated wild-type bacteriorhodopsin as a reference. The features of this last map demonstrate that in the F219L mutant, addition of the light-induced conformational changes to those present prior to illumination results in a net conformational change that is essentially similar in character and in extent to that observed with wild-type bacteriorhodopsin (compare with Figure 2).

Structural changes before and after illumination in other mutants that trap either M or N intermediates

Comparison of the projection maps obtained from wild-type bacteriorhodopsin with those obtained from the D96G, D96N and F219L mutants show that the extent of the light-driven conformational change depends to a considerable extent on the nature of perturbations introduced by the mutation rather than on the optically determined spectroscopic state of the intermediate. This conclusion is further supported by the studies reported below with three other mutants that display slowed photocycles, resulting in the accumulation of M or N intermediates.

Spectroscopic studies with the D38R mutant have shown that decay of the M intermediate is the rate-limiting step in the photocycle (Riesle *et al*., 1996). Like the F219L mutant, small perturbations of the structure are detectable even before illumination (Figure 7(a)). In contrast to the other mutants discussed so far (see for example Figures 4 or 6), there are only small further changes in protein structure upon illumination (Figure 7(b)). Thus, even though the D38R mutant displays a light-driven transition to the M intermediate that is spectroscopically similar to that observed in wild-type bacteriorhodopsin and the Asp96 mutants, it is not accompanied by a large protein conformational change. A similar result was reported recently by Sass *et al*. (1998), based on difference Fourier maps constructed using X-ray powder diffraction data to 7 Å, who showed that light-induced structural changes in this mutant are minimal at pH 6, but much more pronounced at pH 10. Their results, as well as ours, are consistent with the accumulation of the M_1 intermediate (Varo & Lanyi, 1991a) in the photocycle of this mutant at pH 6.

Replacement of Thr46 by Val results in very rapid decay of the M intermediate ($\tau \sim 1$ ms) and accumulation of the N intermediate (Marti *et al*., 1991; Brown *et al*., 1994a). Difference Fourier maps for this mutant show that as in the case of the F219L mutant, there are significant structural changes before illumination (Figure 7(c)) and further significant changes upon illumination (Figure 7(d)). Although the light-induced structural changes bear a general resemblance to those observed with wild-type bacteriorhodopsin and the other mutants, there are noticeable differences in detail, especially in peaks that are in the vicinity of helices B and C.

The D96G/F171C/F219L triple mutant was designed to incorporate three mutations that are individually known to delay the late stages of the bacteriorhodopsin photocycle. As shown in Figure 7(e), a large conformational change is observed in this mutant even before illumination. This structural change, with density changes in the vicinity of helices B, C, F and G displays in projec-

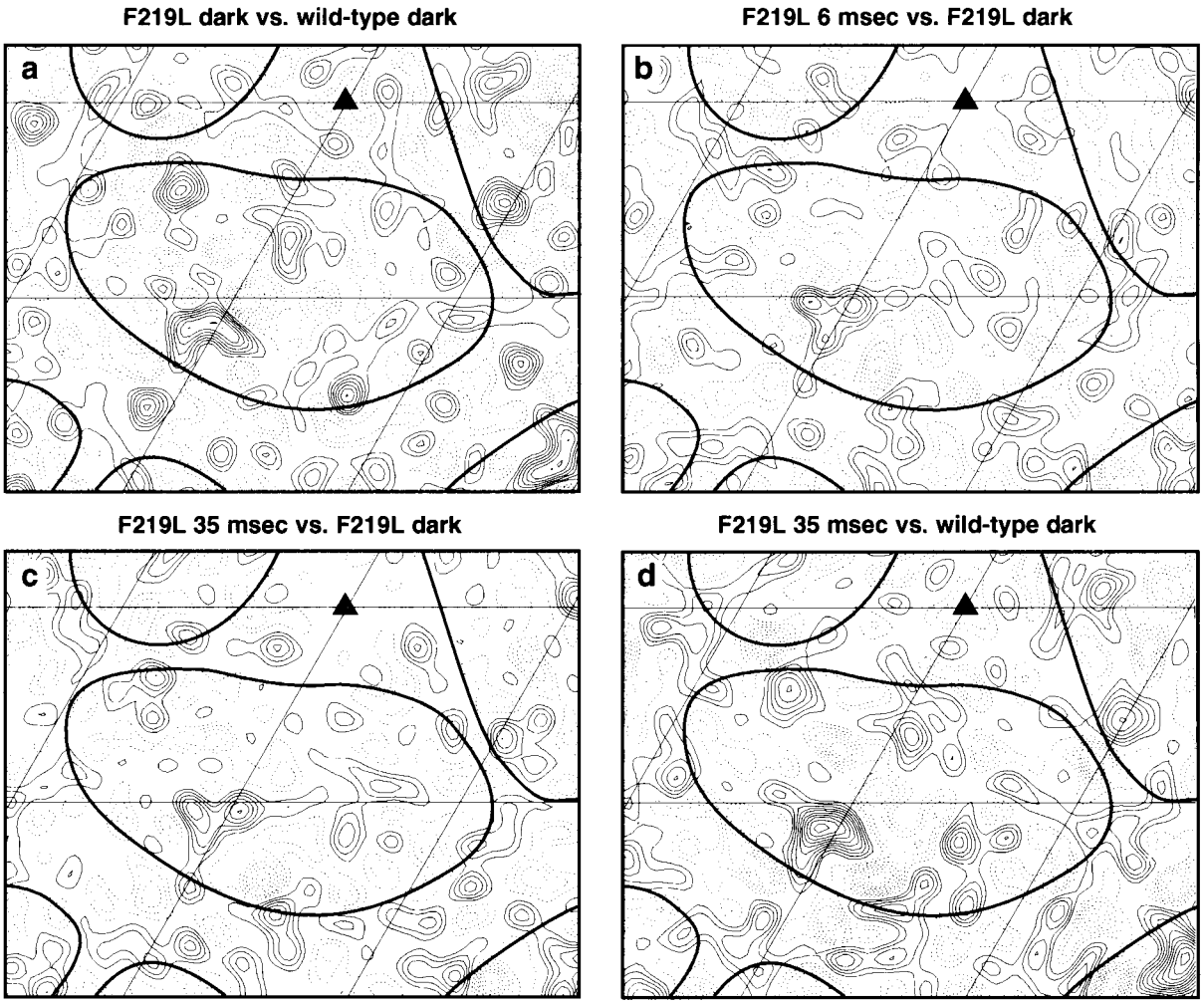

Figure 6. (a) Difference map showing structural changes in unilluminated crystals of the F219L mutant at pH 6.0 and at 5 °C, using unilluminated crystals of wild-type bacteriorhodopsin at pH 6 as a reference. Difference map showing structural changes in crystals of the F219L mutant at pH 6.0 at either (b) 6 ms or (c) 35 ms after illumination using unilluminated crystals of the F219L mutant as a reference. (d) Difference map showing structural changes in crystals of the F219L mutant 35 ms after illumination at pH 6 and at 5 °C using unilluminated crystals of wild-type bacteriorhodopsin at pH 6 as a reference.

tion all of the features seen previously in light-induced structural changes in wild-type bacteriorhodopsin and other mutants. Quantitative analysis of the proton pumping efficiency of the triple mutant relative to wild-type bacteriorhodopsin is underway (J.T. & D.O., unpublished results). Preliminary data suggests that the mutant is capable of light-driven proton translocation, and time-resolved spectroscopic studies show that long-lived M and O intermediates accumulate in the photocycle. However, as in the case of the D38R mutant, only minimal structural changes are observed upon illumination (Figure 7(f)).

Discussion

The most important conclusions from the work presented here can be summarized as follows: (i) Analysis of structural changes in wild-type bacteriorhodopsin reveals that a significant protein conformational change occurs as early as 1 ms after illumination at pH 6. (ii) Small increases in the extent and character of this structural change are observed at higher pH, and at later times in the photocycle, under conditions when a greater accumulation of the N intermediate is expected. (iii) The differences in the structural change between pH 6 and pH 9.5, or between earlier and later times are, however, insufficient to account for the differences seen between structural changes present at the M intermediate stage of the wild-type photocycle, and the N-like (M_N) intermediate of the D96G mutant photocycle. (iv) Structural changes in the D96N mutant are almost identical with those seen in wild-type, suggesting that the Asp96 → Gly mutation results in alteration of the overall conformational flexibility of the protein, and that this effect is not observed with the isosteric Asp96 → Asn replacement. (v) Comparison of structural changes in the F219L mutant at early (M intermediate) and late (N intermediate) stages further confirms that there are only minor global

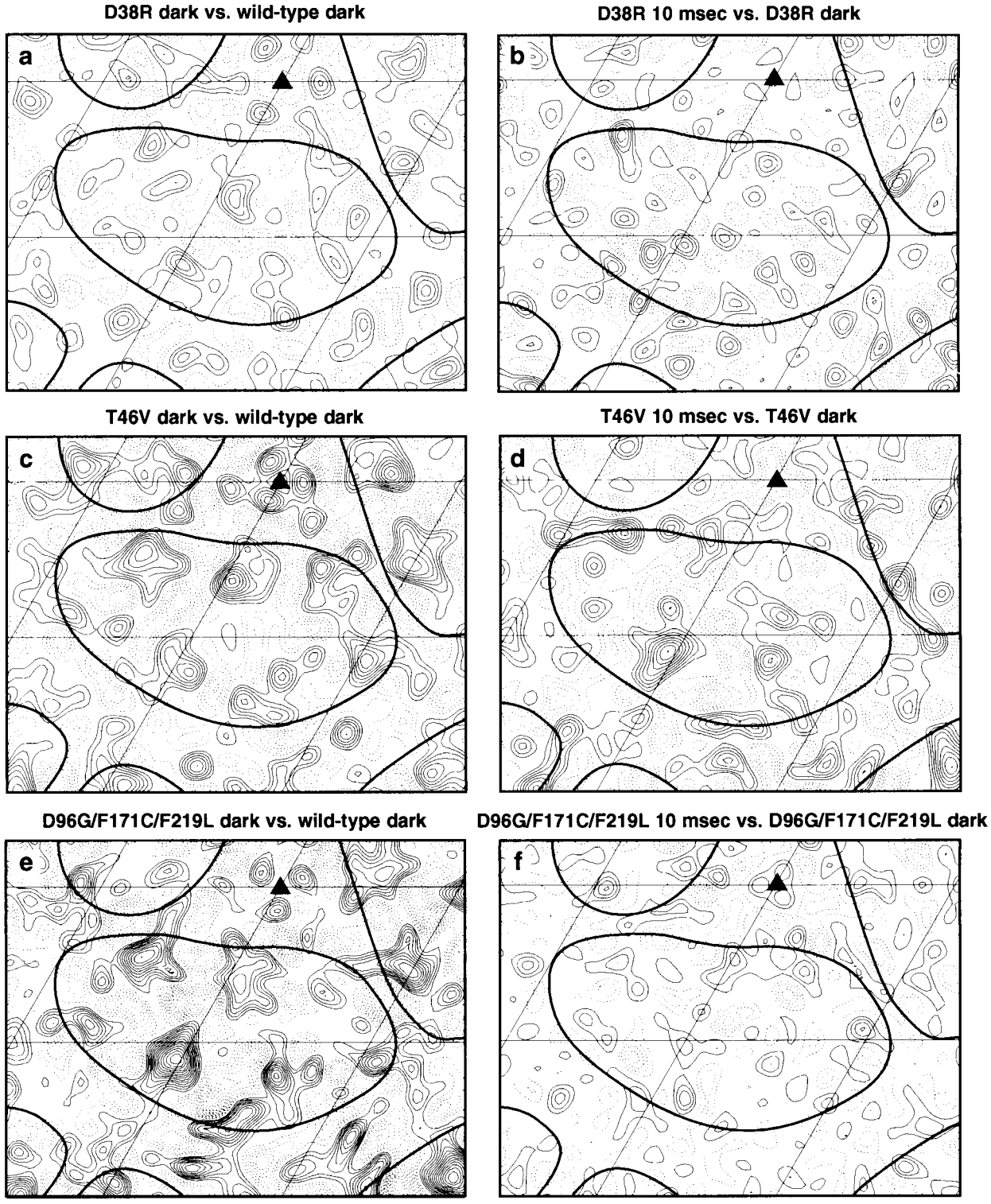

Figure 7. (a) Difference map showing structural changes in unilluminated crystals of the D38R mutant at pH 6 and at 5 °C using unilluminated crystals of wild-type bacteriorhodopsin at pH 6 as a reference. (b) Difference map showing light-induced structural changes in the D38R mutant 10 ms after illumination using unilluminated crystals of the D38R mutant as a reference. (c) Difference map (at 4.2 Å resolution) showing structural changes in unilluminated crystals of the T46V mutant at pH 6 and at 5 °C using unilluminated crystals of wild-type bacteriorhodopsin at pH 6 as a reference. (d) Difference map (at 4.2 Å resolution) showing light-induced structural changes in the T46V mutant 10 ms after illumination using unilluminated crystals of the T46V mutant as a reference. (e) Difference map showing structural changes in unilluminated crystals of the D96G/F171C/F219L triple mutant at pH 6 and at 5 °C using unilluminated crystals of wild-type bacteriorhodopsin at pH 6 as a reference. (f) Difference map showing light-induced structural changes in the D96G/F171C/F219L triple mutant 10 ms after illumination using unilluminated crystals of the triple mutant as a reference.

protein conformational changes associated with the conversion of the M to the N intermediate. (vi) The extent of the light-induced structural changes associated with formation of the M intermediate can be minimal as in the D38R and triple mutants, or considerably larger as in most other mutants, demonstrating that changes in absorption spectrum do not necessarily correlate with global changes in protein conformation. (vii) In many of the mutants studied, there is some detectable perturbation of the unilluminated structure when compared to unilluminated wild-type bacteriorhodopsin. The nature of this structural perturbation depends on the mutation, and in selected instances, the resulting change in conformation in the absence of illumination is comparable both in character and extent to the light-induced structural change in wild-type bacteriorhodopsin.

A number of previous publications have discussed the results of efforts to analyze structural changes in the photocycle using NMR, vibrational and EPR spectroscopic methods, as well as by electron and X-ray diffraction methods. Solid state NMR experiments (Hu *et al*., 1997) using isotopically labeled probes have provided especially useful insights into local environmental changes of selected residues during the photocycle, and are therefore complementary to the electron crystallographic experiments reported here. FTIR spectroscopic studies have identified vibrational spectroscopic features associated with the amide region of the spectrum that are unique to the N intermediate, and are not present in the M intermediate (Braiman *et al*., 1991; Sasaki *et al*., 1992; Souvignier & Gerwert, 1992; Kandori, 1998). It has therefore been inferred that large protein conformational changes may occur upon conversion of the M to the N intermediate (Ludlam & Rothschild, 1997). The observation of significant changes in amide group vibrations between M and N intermediates is not inconsistent with the small changes reported here for global changes in protein conformation between these intermediates. Vibrational spectra are very sensitive to local changes in environment, and in particular to torsional motions or constraints of the peptide backbone. In contrast, the projection difference maps presented here reflect changes in conformation integrated over the length of each helix. While the changes in the vibrational spectrum between the M and N intermediates must undoubtedly be accounted for in a complete mechanistic description of the photocycle, based on the difference Fourier maps presented here, we conclude that these changes cannot reflect large changes in global protein conformation. A similar conclusion was reached by Sass *et al*. (1997), who made parallel X-ray and FTIR measurements in photostationary states at different relative humidities.

From EPR spectroscopic studies using spin labels introduced into the B-C and E-F loop regions of the protein, Steinhoff *et al*. (1994) and Thorgeirsson *et al*. (1997) have concluded that there are essentially no protein structural changes associated with formation of the M intermediate, and that all changes occur upon formation of the N intermediate. The most likely reason that the EPR measurements have not detected the structural changes at the M intermediate stage is that the spin labeling studies have primarily addressed local structural changes in the loop regions of the protein. It is possible that these loop region structural changes are related to the features that we observe in the double difference map comparing structural changes in intermediates trapped at early and late times in the photocycle (Figure 2(f)). However, since these are small compared to the main conformational change, we conclude that the EPR measurements must be sensing either a local change at the surface which is insensitive to the main, large conformational change in structure that occurs within the membrane-embedded portion of bacteriorhodopsin, or that the EPR signal which senses these main changes is somehow delayed in time.

The conclusions from our work are in agreement with the deductions from the analysis of earlier optical spectroscopic data (Lanyi, 1993; Oesterhelt *et al*., 1992) and recent X-ray (Sass *et al*., 1997) and neutron diffraction (Weik *et al*., 1998) studies with the D96N mutant which suggest that the main conformational change in the photocycle occurs on a time-scale when the M intermediate has accumulated. These studies, carried out with oriented two-dimensional crystals, have suggested that the structural change which is observed in the D96N mutant at hydration levels >75% under steady-state illumination is essentially absent at low hydration (<57%). Since light-induced deprotonation of the Schiff base occurs at both lower and higher hydration levels, the implication of these experiments is that the occurrence of the protein structural change correlates with the transition from the M_1 to the M_2 intermediate. Similar results have also been reported by Kamikubo *et al*., (1997), who refer to the hydration-dependent changes as M-type (low hydration) and N-type (high hydration). Irrespective of the nomenclature used, the results from both X-ray diffraction experiments are consistent in general terms with the findings reported in the present work, which has been carried out under fully hydrated conditions and with millisecond time-resolution.

Knowledge of the structures of each of the intermediates in the photocycle will be essential for a complete understanding of the mechanism of proton transport. Although each of these intermediates must have at least subtle differences in conformation from the others, our structural analyses suggest that a simplified view of the photocycle in terms of two principal protein conformations is justified (Figure 8(a)). Efforts to determine structural changes at the K (Bullough & Henderson, 1999) stage of the photocycle by trapping it at $-170\,^{\circ}C$ have shown that there are no significant differences in structure compared to the unilluminated

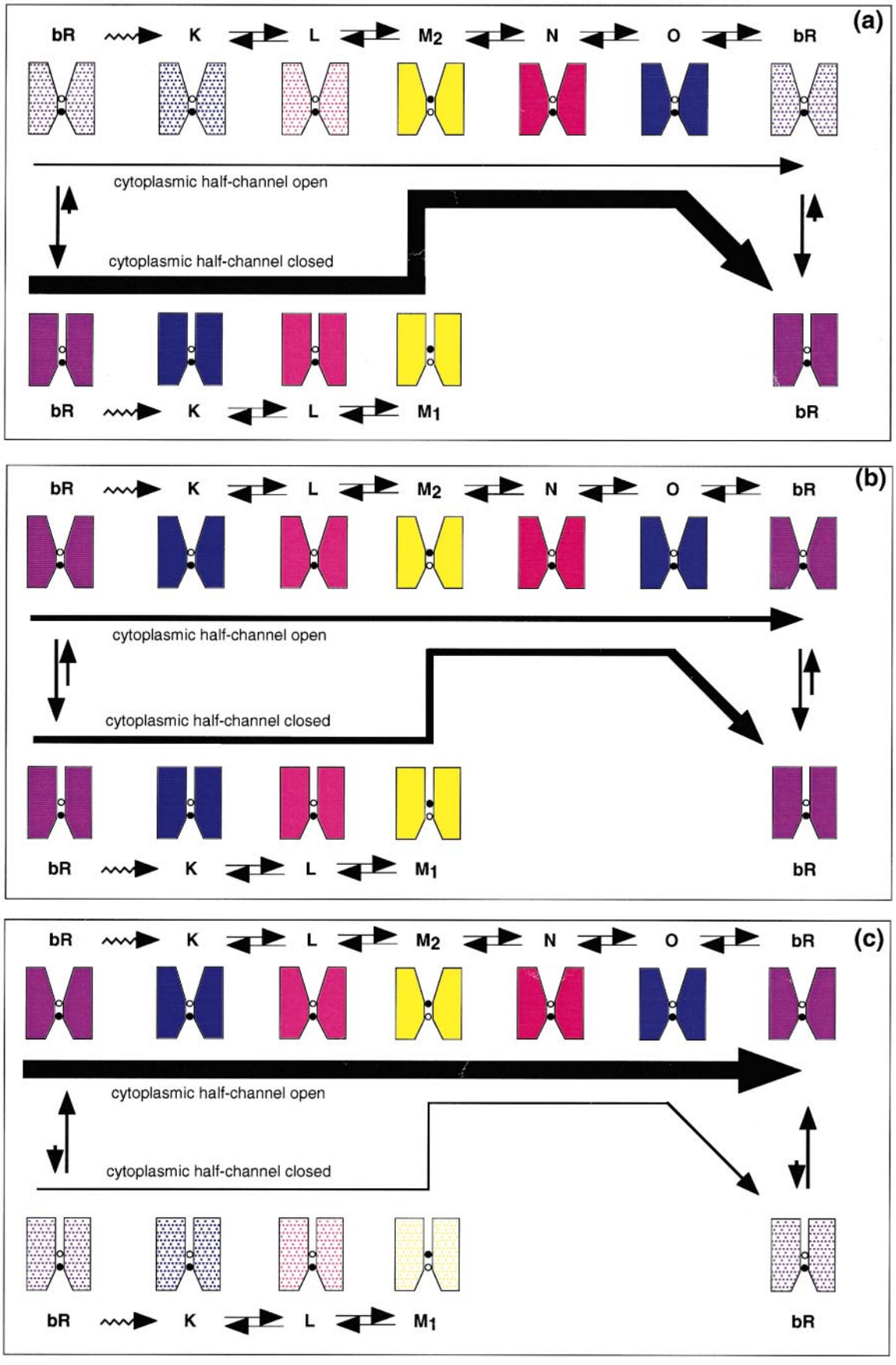

Figure 8 (*legend opposite*)

state of wild-type bacteriorhodopsin. Hendrickson *et al*. (1998) have carried out similar experiments aimed at trapping the L intermediate (at −100 °C), and have reported that there are no detectable structural changes at this stage of the photocycle. The results from the X-ray and neutron diffraction studies at low humidity (Sass *et al*., 1997; Kamikubo *et al*., 1997; Weik *et al*., 1998) clearly show that there is no evidence for a structural change at the M_1 stage of the photocycle. We therefore conclude that the structures of the initial unilluminated state and those of the early intermediates (K, L and M_1) are likely to be well-approximated by one conformation, in which the Schiff base is preferentially accessible to the extracellular side. From the present work and the results reported in Subramaniam *et al*. (1997), we conclude that the structures of the other intermediates (M_2, N, and the 13-*cis* O intermediate) are well-approximated by the other conformation, in which the Schiff base is preferentially accessible to the cytoplasmic side. In wild-type bacteriorhodopsin, and in several mutants, the main structural change in the photocycle occurs with the formation of the M_2 intermediate. This structural change is reversed in the final stage of the photocycle, corresponding to the decay of the N and O intermediates back to the initial bacteriorhodopsin state. In selected mutants, a partial conformational change is already present before illumination. The full extent of the conformational change is obtained upon illumination, even though the two components, i.e. the conformational change in the unilluminated state and the change occurring upon the light-driven formation of the M (or N) intermediate do not bear a direct resemblance to each other (Figure 8(b)). Finally, in the D96G/F171C/F219L triple mutant, the conformation of the protein is almost completely shifted in favor of the conformation that is only observed upon illumination in wild-type bacteriorhodopsin (Figure 8(c)).

A similar example has been previously reported in the case of the D85N single mutant and the D85N/D96N double mutant, where substantial protein conformational changes in the vicinities of helices F and G are observed even in the absence of illumination (Kataoka *et al*., 1994; Brown *et al*., 1994b; Lindahl & Henderson, 1997).

Since there is a large variation in the extent of the light-driven protein conformational change in the different mutants, what can be concluded about the nature of the ''switch'' that accounts for the change in proton accessibility of the Schiff base from the extracellular side to the cytoplasmic side? Is the large protein conformational change essential for switching accessibility of the Schiff base? Is there a role for subtler, and as yet unobserved structural changes in retinal and/or the protein that are the heart of the mechanism of proton pumping? Since the triple mutant can function as a

Figure 8. Schematic description of conformational changes in wild-type bacteriorhodopsin and the various mutants studied in this work. It is proposed that in all cases, the unilluminated state of the protein is best described as an equilibrium mixture between two conformations. In one, the Schiff base is primarily accessible to the extracellular side, and in the other, primarily to the cytoplasmic side. In each panel, the predominant conformation of each photocycle intermediate is shown in filled color, whereas the minor conformation is shown with stippled coloring. (a) In unilluminated wild-type bacteriorhodopsin, the equilibrium is shifted largely towards the conformation which has accessibility to the extracellular side. Upon illumination, retinal is isomerized, followed by deprotonation of the Schiff base, and the equilibrium is then shifted to favor the conformation that has accessibility to the cytoplasmic side. The change in accessibility of the Schiff base is indicated, in part, by an ''opening'' of the protein to the cytoplasmic side. The purpose of showing the opening is to conceptually highlight the protein contribution to the change in accessibility, and should not be taken to imply an associated large influx of water from the cytoplasmic side. Similarly, the retinal component of the change in accessibility is indicated schematically by the change in ''fill'' pattern in the pair of circles in the center of the protein. In intermediates where the Schiff base is protonated, the Schiff's base nitrogen atom (filled circle) is in the position closer to the extracellular side. In the deprotonated Schiff base intermediates, the nitrogen atom is in a position closer to the cytoplasmic side. Such a change in position could occur upon a deprotonation-induced decrease in curvature of retinal (S.S. & R.H., unpublished results), providing an explanation for preferential reprotonation of the unprotonated Schiff base *via* the cytoplasmic half-channel. Following re-protonation of the Schiff base, and the thermal re-isomerization of retinal, the equilibrium is shifted back in favor of the conformation that has accessibility to the extracellular side. For simplicity, the protein structural change is shown here as being reversed with the decay of the O intermediate. While we have shown before that the structural change is still present in the 13-*cis* O intermediate, it is possible that the structural change is already reversed upon formation of the all-*trans* O intermediate. (b) In mutants such as T46V, L93A, or F219L, the equilibrium is partially shifted even in the unilluminated state towards the conformation that has accessibility to the cytoplasmic side. Upon illumination, the equilibrium shifts completely to this state. Since the features of the conformational change in the unilluminated state are somewhat different from those observed upon illumination, the postulate about cytoplasmic accessibility in the unilluminated state of these single mutants remains to be tested. As in the case of wild-type bacteriorhodopsin, it is expected that structural changes in both retinal and the protein contribute to the ''switch'' in accessibility that is required for light-driven proton transport. However, in these mutants, it is likely that there is a smaller relative contribution from the protein as compared to the case of wild-type bacteriorhodopsin. (c) In the D96G/F171C/F219L triple mutant, the equilibrium is almost completely shifted in the unilluminated state towards the conformation that has accessibility primarily to the cytoplasmic side. Only minimal further changes occur with illumination. It is therefore likely that in this triple mutant, structural changes in retinal provide most of the contribution to the light-induced switch in accessibility.

proton pump, it follows that a switch in accessibility of the Schiff base can occur even in the absence of a significant light-induced protein conformational change in the cytoplasmic half of the membrane at the 3.5 Å resolution of our difference maps (Figure 7(f)). Hence, in this mutant, the molecular origin of the switch must reside in subtle structural rearrangements in retinal and/or the protein that are triggered by light absorption. Given the central location and importance of the retinylidene Schiff base in proton pumping, it is most likely that this subtler component is constituted by structural changes localized on the retinal moiety.

If indeed there are changes in retinal that constitute the ''switch'' it is necessary that they occur between the L state where the Schiff base accessibility is extracellular and the M_2 state where the Schiff base accessibility is cytoplasmic (see Figure 8(c)). Further, the nature of this change must be to displace the Schiff base nitrogen atom from a position that is connected or proximal to the extracellular half-channel to a position that is connected or proximal to the cytoplasmic half-channel. Schulten & Tavan (1978) proposed that such a repositioning could occur as a consequence of rotation around the C14—C15 single bond following retinal-isomerization around the C13=C14 double bond. This model is, however, not supported by the Resonance Raman studies by Fodor *et al*. (1988) who showed that the configuration of retinal remains 13-*cis*, 15-*anti* in both L and N intermediates, which occur on different sides of the ''accessibility switch''. An alternative model for displacement of the Schiff base nitrogen atom derives from an analysis (S.S. & R.H., unpublished results) of the spectroscopic properties and crystal structures of a number of retinylidene compounds, which indicates a reduction in the curvature of retinal upon deprotonation of the Schiff base. Such a decreased curvature is in the right direction to contribute to the observed change in accessibility, since it should result in a displacement of the Schiff base nitrogen atom towards the cytoplasm. If neither of the above models is confirmed by experiment, a third possibility is that single-bond, out-of-plane rotations of retinal reposition the Schiff base following deprotonation. How such a movement could generate the required change in accessibility, is, however, not clear.

None of the mutants analyzed in this work involve amino acid replacements that are in the immediate vicinity of the Schiff base. We therefore expect that irrespective of the nature of any retinal structural change between the L and M_2 intermediates, deprotonation-induced repositioning of the Schiff base will contribute to the overall switching action that is required for vectorial proton transport in wild-type bacteriorhodopsin as well as in all the mutants studied. In wild-type bacteriorhodopsin, there is no definitive evidence yet for or against the contribution of the large protein conformational change to the switch in accessibility. However, because of its cytoplasmic location, and inferred ''opening'' of the protein structure (Subramaniam *et al*., 1993), we expect that light-induced protein conformational changes are likely to make an additional contribution to the switch. In mutants where there is already a partial conformational change before illumination, we expect that there would be smaller additional contributions from the protein conformational change than in wild-type bacteriorhodopsin, while in the case of the D96G/F171C/F219L triple mutant, as discussed above, contributions from the protein component of the switch would be minimal. A full understanding of the molecular basis of proton transport now awaits biophysical experiments that can quantitatively dissect the relative contributions of structural changes in retinal and the protein to the switch in accessibility, and structural experiments that will provide an atomic description of the main protein conformational change that we have analyzed here.

Methods

Preparation of crystalline patches of bacteriorhodopsin

Purple membranes containing either wild-type bacteriorhodopsin or various mutants were isolated from *H. salinarium* as described (Oesterhelt & Stoeckenius, 1974; Ferrando *et al*., 1993). The isolated membranes, which were typically 0.5 to 1.0 mm in size, were then fused in the presence of octyl glucoside and DTAC as described (Baldwin & Henderson, 1984) to obtain larger crystalline patches with an average size of ~5 μm).

Preparation of specimens for microscopy

Samples were processed for electron microscopy essentially as described by Subramaniam *et al*. (1993). A 3 μl sample of a suspension of fused membranes was deposited on carbon-coated electron microscopic grids, pretreated with 1 μl of 1 % (w/v) octyl glucoside at pH 7. The pH of the droplet on the grid was measured to be ~ 6.0. In experiments where intermediates were trapped at alkaline pH, 2 μl of the fused membranes were mixed with an appropriate volume of 1 M sodium bicarbonate buffer at pH 10 for a final concentration of 0.7 M carbonate and a final pH of 9.5. The specimen was inserted into a temperature-controlled environmental chamber designed by Dr Y. Talmon and colleagues (Bellare *et al*., 1988) and blotted with Whatman no. 1 filter paper to remove excess liquid. To determine changes in the unilluminated state, the fully hydrated grids (typically at ~5 °C) were plunged at speed of 2 to 9 m/second into liquid ethane following a dark adaptation period, typically about three minutes in duration. To trap intermediates, the suspension on the grid was first light-adapted with several flashes of illumination before being inserted into the environmental chamber. Following blotting , and while the grid was in transit towards the surface of the liquid ethane, it was illuminated with a flash of light ($\lambda > 570$ nm) to initiate the photocycle. The duration of the light flash was ~1 ms, with an intensity that was sufficient to excite most (>80 %) of the bacteriorhodopsin molecules on the grid.

In experiments where intermediates were trapped at times >5 ms after illumination, the speed of the spring-based plunger was ~2 m/second as described in our earlier work. For trapping intermediates at earlier times, a pneumatically driven plunger was constructed based on a design previously developed by Drs J. Trinick and H. White at Bristol University (White *et al*., 1998). Grids held at the end of this plunger could be propelled at speeds of up to 9 m/second, as monitored using a photodiode assembly connected to a digital oscilloscope. At the highest speed, the transit time of the grids across the flash was ~0.3 ms, since the radius of the circular grids used in our experiments is ~1.5 mm. All crystals on the grid were illuminated simultaneously since the width of the illuminating beam in the plane of the falling grid was set to be ~10 mm wide. To obtain the shortest possible delay times, grids were illuminated at a distance of ~6 mm above the surface of the liquid ethane to give a maximal delay of ~ 0.8 ms between the flash and time when the grid contacted the surface of the liquid ethane. It has been estimated that the specimens on copper grids are cooled at a rate >100,000 K/second following the plunge into liquid ethane (Mayer & Astl, 1992; Berriman & Unwin, 1994). At this freezing rate, a temperature drop of 20 °C will therefore occur within 0.2 ms. This additional delay is a reasonable estimate to account for the time over which any further evolution of the conformational change may occur, since it is known that a five-fold reduction in the rate of decay of the M intermediate requires a temperature drop of about 20 °C (Varo & Lanyi, 1991b; Delaney *et al*., 1995). We therefore obtain an estimate of ~1 ms for the total delay between the ''flash'' and ''freeze'' events under the conditions of our experiment. Once frozen, the grids were transferred from liquid ethane into liquid nitrogen. All subsequent manipulations of the sample were carried out at liquid nitrogen temperatures.

Recording of diffraction patterns and construction of Fourier difference maps

The specimens were analyzed at liquid nitrogen temperatures using a Philips CM-12 microscope operating at 120 kV. Diffraction patterns were collected with the aid of a CCD detector (Faruqi *et al*., 1995, 1998), and processed using previously described methods (Baldwin & Henderson 1984). Difference Fourier maps were obtained using phases for bacteriorhodopsin reported in Grigorieff *et al*. (1996). Typically, structure factors averaged from diffraction patterns of six to ten illuminated crystals and six to ten unilluminated crystals were used in construction of the difference map. Unless otherwise noted, all difference maps are plotted at 3.5 Å resolution.

Acknowledgements

We thank Drs John Trinick and Howard White for providing us with details of their apparatus to propel grids at high speeds using a pneumatic plunger, and Mick Fordham for his help in constructing the apparatus. This work was supported in part by grants to S.S. from the Fogarty Senior International Fellowship, and the National Eye Institute (while at the Johns Hopkins University School of Medicine, Baltimore) and an EMBO fellowship to M.L.

References

Ames, J. B. & Mathies, R. A. (1990). The role of back-reactions and proton uptake during the N → O transition in bacteriorhodopsin's photocycle: a kinetic resonance Raman study. *Biochemistry,* **29**, 7181-7190.

Baldwin, J. & Henderson, R. (1984). Measurement and evaluation of electron diffraction patterns from two-dimensional crystals. *Ultramicroscopy,* **14**, 319-336.

Bellare, J., Davis, H. T., Scriven, L. E. & Talmon, Y. (1988). Controlled environment vitrification system: An improved sample preparation technique. *J. Electr. Micros. Techn.* **10**, 87-111.

Berriman, J. & Unwin, N. (1994). Analysis of transient structures by cryomicroscopy combined with rapid mixing of spray droplets. *Ultramicroscopy,* **56**, 241-252.

Braiman, M. S., Bousche, O. & Rothschild, K. J. (1991). Protein dynamics in the bacteriorhodopsin photocycle: submillisecond Fourier transform infrared spectra of the L, M and N-photointermediates. *Proc. Natl Acad. Sci. USA,* **88**, 2388-2392.

Brown, L. S., Yamazaki, Y., Maeda, A., Sun, L., Needleman, R. & Lanyi, J. K. (1994a). The proton transfers in the cytoplasmic domain of bacteriorhodopsin are facilitated by a cluster of interacting residues. *J. Mol. Biol.* **239**, 401-414.

Brown, L. S., Kamikubo, H., Zimanyi, L., Kataoka, M., Tokunaga, F., Verdegem, P., Lugtenberg, J. & Lanyi, J. K. (1994b). A local electrostatic change is the cause of the large scale protein conformational shift in bacteriorhodopsin. *Proc. Natl Acad. Sci. USA,* **94**, 5040-5044.

Bullough, P. & Henderson, R. (1999). The projection structure of the K intermediate of the bacteriorhodopsin photocycle determined by electron diffraction. *J. Mol. Biol.* **286**, 1661-1669.

Butt, H. J., Fendler, K., Bamberg, E., Tittor, J. & Oesterhelt, D. (1989). Aspartic acids 96 and 85 play a central role in the function of bacteriorhodopsin as a proton pump. *EMBO J.* **8**, 1657-1663.

Delaney, J. K., Schweiger, U. & Subramaniam, S. (1995). Molecular mechanism of protein-retinal coupling in bacteriorhodopsin. *Proc. Natl Acad. Sci. USA,* **92**, 11120-11124.

Dencher, N. A., Dresselhaus, D., Zaccai, G. & Büldt, G. (1989). Structural changes in bacteriorhodopsin during proton translocation revealed by neutron diffraction. *Proc. Natl Acad. Sci. USA,* **86**, 7876-7879.

Ebrey, T. G. (1993). Light energy transduction in bacteriorhodopsin. In *Thermodynamics of Membrane Receptors and Channels* (Jackson, M., ed.), pp. 353-387, CRC Press, Boca Raton, FL.

Faruqi, A. R., Andrews, H. N. & Henderson, R. (1995). A high sensitivity imaging detector for electron microscopy. *Nucl. Instr. Methods Phys. Res. ser. A,* **367**, 408-412.

Faruqi, A. R., Henderson, R. & Subramaniam, S. (1999). *Ultramicroscopy,* **75**, 235-250.

Ferrando, E., Schweiger, U. & Oesterhelt, D. (1993). Homologous bacterio-opsin encoding gene expression via site-specific vector integration. *Gene,* **125**, 41-47.

Fodor, S. P., Ames, J. B., Gebhard, R., van der Berg, E. M., Stoeckenius, W., Lugtenburg, J. & Mathies, R. A. (1988). Chromophore structure in bacteriorhodopsin's N intermediate: implications for the proton pumping mechanism. *Biochemistry,* **27**, 7097-7101.

Gerwert, K., Hess, B., Soppa, D. & Oesterhelt, D. (1989). Role of aspartate-96 in proton translocation by bacteriorhodopsin. *Proc. Natl Acad. Sci. USA,* **86**, 4943-4947.

Grigorieff, N., Ceska, T., Downing, K. H., Baldwin, J. M. & Henderson, R. (1996). Electron crystallographic refinement of the structure of bacteriorhodopsin. *J. Mol. Biol.* **259**, 393-421.

Grzesiek, S. & Dencher, N. A. (1986). Time-course and stoichiometry of light-induced proton release and uptake during the photocycle of bacteriorhodopsin. *FEBS Letters,* **208**, 337-342.

Hendrickson, F. M., Burkard, F. & Glaeser, R. M. (1998). Structural characterization of the L-to-M transition of the bacteriorhodopsin photocycle. *Biophys. J.* **75**, 1446-1454.

Hu, J. G., Boqin, Q. S., Petkova, A. T., Griffin, R. G. & Herzfeld, J. (1997). The predischarge chromophore in bacteriorhodopsin: A ^{15}N solid-state NMR study of the L photointermediate. *Biochemistry,* **36**, 9316-9322.

Kamikubo, H., Kataoka, M., Varo, G., Oka, T., Tokunaga, F., Needleman, R. & Lanyi, J. K. (1996). Structure of the N-intermediate of bacteriorhodopsin revealed by X-ray diffraction. *Proc. Natl Acad. Sci. USA,* **93**, 1386-1390.

Kamikubo, H., Oka, T., Imamoto, Y., Tokunaga, F., Lanyi, J. K. & Kataoka, M. (1997). The last phase of the reprotonation switch in bacteriorhodopsin: The transition between the M-type and the N-type protein conformation depends on hydration. *Biochemistry,* **36**, 12282-12287.

Kandori, H. (1998). Polarized FTIR spectroscopy distinguishes peptide backbone changes in the M and N photointermediates of bacteriorhodopsin. *J. Am. Chem. Soc.* **120**, 4546-4547.

Kandori, H., Yamazaki, Y., Hatanaka, M., Needleman, R., Brown, L. S., Richter, H. T., Lanyi, J. K. & Maeda, A. (1997). Time-resolved Fourier transform infrared study of structural changes in the last steps of the photocycles of Glu-204 and Leu-93 mutants of bacteriorhodopsin. *Biochemistry,* **36**, 5134-5141.

Kataoka, M., Kamikubo, H., Tokunaga, F., Brown, L. S., Yamazaki, Y., Maeda, A., Sheves, M., Needleman, R. & Lanyi, J. K. (1994). Energy coupling in an ion pump: the reprotonation switch of bacteriorhodopsin. *J. Mol. Biol.* **243**, 621-638.

Koch, M. H. J., Dencher, N., Oesterhelt, D., Plöhn, H.-J., Rapp, G. & Büldt, G. (1991). Time-resolved X-ray diffraction study of structural changes associated with the photocycle of bacteriorhodopsin. *EMBO J.* **10**, 521-526.

Lanyi, J. K. (1993). Proton translocation mechanism and energetics in the light-driven pump bacteriorhodopsin. *Biochim. Biophys. Acta,* **1183**, 241-261.

Lindahl, M. & Henderson, R. (1998). Structure of the bacteriorhodopsin D85N/D96N double mutant showing substantial structural changes and a highly twinned, disordered lattice. *Ultramicroscopy,* **70**, 95-106.

Lozier, R. H., Bogomolni, R. A. & Stoeckenius, W. (1975). Bacteriorhodopsin: a light-driven proton pump in *Halobacterium Halobium*. *Biophys. J.* **15**, 955-963.

Ludlam, G. J. & Rothschild, K. J. (1997). Similarity of bacteriorhodopsin structural changes triggered by chromophore removal and light-driven proton transport. *FEBS Letters,* **407**, 285-288.

Marinetti, T., Subramaniam, S., Mogi, T., Marti, T. & Khorana, H. G. (1989). Replacement of aspartic residues 85, 96, 115, or 212 affects the quantum yield and kinetics of proton release and uptake by bacteriorhodopsin. *Proc. Natl Acad. Sci. USA,* **86**, 529-533.

Marti, T., Otto, H., Mogi, T., Rösselet, S., Heyn, M. P. & Khorana, H. G. (1991). Bacteriorhodopsin mutants containing single substitutions of serine or threonine residues are all active in proton translocation. *J. Biol. Chem.* **266**, 6919-6927.

Mayer, E. & Astl, G. (1992). Limits of cryofixation as seen by Fourier transform infrared spectra of metmyoglobin azide and carbonyl hemoglobin in vitrified and freeze concentrated aqueous solution. *Ultramicroscopy,* **45**, 185-197.

Miller, A. & Oesterhelt, D. (1990). Kinetic optimization of bacteriorhodopsin by aspartic acid 96 as an internal proton donor. *Biochim. Biophys. Acta,* **1020**, 57-64.

Oesterhelt, D. & Stoeckenius, W. (1974). Isolation of cell membrane of *Halobacterium halobium* and its fractionation into red and purple membrane. *Methods Enzymol.* **31**, 667-678.

Oesterhelt, D., Tittor, J. & Bamberg, E. (1992). A unifying concept for ion translocation by retinal proteins. *J. Bioenerg. Biomemb.* **24**, 181-191.

Otto, H., Mareti, T., Holz, M., Mogi, T., Lindau, M., Khorana, H. G. & Heyn, M. P. (1989). Aspartic acid 96 is the internal proton donor in the reprotonation of the Schiff base of bacteriorhodopsin. *Proc. Natl Acad. Sci. USA,* **86**, 9228-9232.

Otto, H., Mareti, T., Holz, M., Mogi, T., Stern, L. J., Engel, F., Khorana, H. G. & Heyn, M. P. (1990). Substitution of amino acids Asp-85, Asp-212 and Arg-82 in bacteriorhodopsin affects the proton release of the pump and the pK of the Schiff base. *Proc. Natl Acad. Sci. USA,* **87**, 1018-1022.

Pfefferle, J.-M., Maeda, A., Sasaki, J. & Yoshizawa, Y. (1991). Fourier Transform infrared study of the N intermediate of bacteriorhodopsin. *Biochemistry,* **30**, 6548-6556.

Rammelsberg, R., Huhn, G., Lübben, M. & Gerwert, K. (1998). Bacteriorhodopsin's intramolecular proton-release pathway consists of a hydrogen-bonded network. *Biochemistry,* **37**, 5001-5009.

Riesle, J., Oesterhelt, D., Dencher, N. & Heberle, J. (1996). D38 is an essential part of the proton translocation pathway in bacteriorhodopsin. *Biochemistry,* **35**, 6635-6643.

Sasaki, J., Schichida, Y., Lanyi, J. K. & Maeda, A. (1992). Protein changes associated with reprotonation of the Schiff base in the photocycle of Asp 96 → Asn bacteriorhodopsin: the M_N intermediate with unprotonated Schiff base but N-like protein. *J. Biol. Chem.* **267**, 20782-20786.

Sass, H. J., Schachowa, I. W., Rapp, G., Koch, M. H. J., Oesterhelt, D., Dencher, N. A. & Büldt, G. (1997). The tertiary structural changes in bacteriorhodopsin occur between M states: X-ray diffraction and Fourier transform infrared spectroscopy. *EMBO J.* **16**, 1484-1491.

Sass, H. J., Gessenich, R., Koch, M. H. J., Oesterhelt, D., Dencher, N. A., Büldt, G. & Rapp, G. (1998). Evidence for charge-controlled conformational changes in the photocycle of bacteriorhodopsin. *Biophys. J.* **75**, 399-405.

Schulten, K. & Tavan, P. (1978). A mechanism for the light-driven proton pump of *Halobacterium halobium*. *Nature,* **272**, 85-86.

Smith, S. O., Pardoen, J. A., Mulder, P. P. J., Curry, B., Lugtenburg, J. & Mathies, R. A. (1983). Chromophore structure in bacteriorhodopsin's O_{640} photointermediate. *Biochemistry,* **22**, 6141-6148.

Souvignier, G. & Gerwert, K. (1992). Proton uptake mechanism of bacteriorhodopsin as determined by time-resolved stroboscopic-FTIR-spectroscopy. *Biophys. J.* **63**, 1393-1405.

Steinhoff, H.-J., Mollaaghababa, R., Altenbach, C., Hideg, K., Krebs, M., Khorana, H. G. & Hubbell, W. (1994). Time-resolved detection of structural changes during the photocycle of spin-labeled bacteriorhodopsin. *Science,* **266**, 105-107.

Stoeckenius, W., Lozier, R. H. & Bogomolni, R. A. (1979). Bacteriorhodopsin and related pigments of halobacteria. *Biochim. Biophys. Acta,* **505**, 215-278.

Subramaniam, S., Marti, T. & Khorana, H. G. (1990). Protonation state of Asp (Glu)-85 regulates the purple-to-blue transition in bacteriorhodopsin mutants Arg82 → Ala and Asp85 → Glu: the blue form is inactive in proton translocation. *Proc. Natl Acad. Sci. USA,* **87**, 1013-1017.

Subramaniam, S., Gerstein, M., Oesterhelt, D. & Henderson, R. (1993). Electron diffraction analysis of structural changes in the photocycle of bacteriorhodopsin. *EMBO J.* **12**, 1-8.

Subramaniam, S., Faruqi, A. R., Oesterhelt, D. & Henderson, R. (1997). Electron diffraction studies of light-induced conformational changes in the Leu-93 → Ala bacteriorhodopsin mutant. *Proc. Natl Acad. Sci. USA,* **94**, 1767-1772.

Thorgeirsson, T. E., Xiao, W. Z., Brown, L. S., Needleman, R., Lanyi, J. K. & Shin, Y. K. (1997). Transient channel-opening in bacteriorhodopsin: an EPR study. *J. Mol. Biol.* **273**, 951-957.

Tittor, J., Soell, C., Oesterhelt, D., Butt, H.-J. & Bamberg, E. (1989). A defective proton pump, point-mutated bacteriorhodopsin Asp 96 → Asn is fully re-activated by azide. *EMBO J.* **8**, 3477-3482.

Tsuda, M., Glaccum, M., Nelson, B. & Ebrey, T. G. (1980). Light isomerizes the chromophore of bacteriorhodopsin. *Nature,* **287**, 351-353.

Varo, G. & Lanyi, J. K. (1991a). Kinetic and spectroscopic evidence for an irreversible step between deprotonation and reprotonation of the Schiff base in the bacteriorhodopsin photocycle. *Biochemistry,* **30**, 5008-5015.

Varo, G. & Lanyi, J. K. (1991b). Thermodynamics and energy coupling in the bacteriorhodopsin photocycle. *Biochemistry,* **30**, 5016-5022.

Vonck, J. (1996). A 3-Dimensional difference map of the N-intermediate in the bacteriorhodopsin photocycle: Part of the F-helix tilts in the M-to-N transition. *Biochemistry,* **35**, 5870-5878.

Weik, M., Zaccai, G., Dencher, N. A. & Oesterhelt, D. (1998). Structure and hydration of the M-state of the bacteriorhodopsin mutant D96N studied by neutron diffraction. *J. Mol. Biol.* **275**, 625-634.

White, H. D., Walker, M. L. & Trinick, J. (1998). A computer-controlled spraying-freezing apparatus for millisecond time-resolution electron cryomicroscopy. *J. Struct. Biol.* **121**, 306-313.

Edited by B. Honig

(Received 11 August 1998; received in revised form 19 January 1999; accepted 25 January 1999)